Published in final edited form as:
Magn Reson Imaging. 2012 November ; 30(9): 1342–1356. doi:10.1016/j.mri.2012.06.001.

Simultaneous PET-MRI in Oncology: A Solution Looking for a Problem?

Thomas E. Yankeelov[1,2,3,4,5], **Todd E. Peterson**[1,2,3], **Richard G. Abramson**[1,2], **David Garcia-Izquierdo**[9,10], **Lori R. Arlinghaus**[1,2], **Xia Li**[1,2], **Nkiruka C. Atuegwu**[1,2], **Ciprian Catana**[8], **H. Charles Manning**[1,2,4,6], **Zahi A. Fayad**[9,10,11], and **John C. Gore**[1,2,3,4,7]

[1]Institute of Imaging Science, Vanderbilt University, Nashville, Tennessee, USA

[2]Departments of Radiology and Radiological Sciences, Vanderbilt University, Nashville, Tennessee, USA

[3]Physics and Astronomy, Vanderbilt University, Nashville, Tennessee, USA

[4]Biomedical Engineering, Vanderbilt University, Nashville, Tennessee, USA

[5]Cancer Biology, Vanderbilt University, Nashville, Tennessee, USA

[6]Neurosurgery, Vanderbilt University, Nashville, Tennessee, USA

[7]Molecular Physiology and Biophysics, Vanderbilt University, Nashville, Tennessee, USA

[8]Athinoula A. Martinos Center for Biomedical Imaging, Department of Radiology Massachusetts General Hospital and Harvard Medical School Charlestown, Massachusetts, USA

[9]Translational and Molecular Imaging Institute, Mt. Sinai Medical Center, New York, New York, USA

[10]Departments of Radiology, Mt. Sinai Medical Center, New York, New York, USA

[11]Departments of Cardiology, Mt. Sinai Medical Center, New York, New York, USA

Abstract

With the recent development of integrated positron emission tomography-magnetic resonance imaging (PET-MRI) scanners, new possibilities for quantitative molecular imaging of cancer are realized. However, the practical advantages and potential clinical benefits of the ability to record PET and MRI data simultaneously must be balanced against the substantial costs and other requirements of such devices. In this review we highlight several of the key areas where integrated PET-MRI measurements, obtained simultaneously, are anticipated to have a significant impact on clinical and/or research studies. These areas include the use of MR-based motion corrections and/or *a priori* anatomical information for improved reconstruction of PET data; improved arterial input function characterization for PET kinetic modeling; the use of dual-modality contrast agents; and patient comfort and practical convenience. For widespread acceptance, a compelling case could be made if the combination of quantitative MRI and specific PET biomarkers significantly improves our ability to assess tumor status and response to therapy, and some likely candidates are

Please address correspondence to: Thomas E. Yankeelov, Ph.D., Vanderbilt University Institute of Imaging Science, Vanderbilt University Medical Center, AA-1105 Medical Center North, 1161 21st Avenue South, Nashville, Tennessee 37232-2310, thomas.yankeelov@vanderbilt.edu.

now emerging. We consider the relative advantages and disadvantages afforded by PET-MRI and summarize current opinions and evidence as to the likely value of PET-MRI in the management of cancer.

Keywords

PET; MRI; attenuation; motion; reconstruction; AIF; multi-modality

I. Introduction

The primary cross-sectional medical imaging technologies currently employed in clinical oncology include magnetic resonance imaging (MRI), computed tomography (CT), positron emission tomography (PET), single photon emission computed tomography (SPECT), and ultrasound (US). In recent years there have been dramatic increases in the range and quality of information available from these non-invasive methods so that many potentially valuable imaging metrics are now available to assist in diagnosis, determine extent of disease, measure tumor size, and predict treatment response [see, e.g., 1]. Depending on the modality, quantitative information can be obtained that reports on anatomical (MRI, CT, US), physiological (MRI, CT, PET, US), cellular (MRI, PET), and even molecular (MRI, PET, SPECT, US) events. (Accessible reviews on how each modality contributes to basic and clinical cancer research can be found in, e.g., refs. [2,3].) Each modality offers advantages and trade-offs in, for example, spatial resolution, temporal resolution, sensitivity, signal-to-noise, contrast-to-noise, and ability for quantification. As different modalities have different strengths and weaknesses, there is no one “ideal” technique. This realization has resulted in attempts to integrate complementary imaging approaches synergistically to increase the information yielded beyond single modalities.

In its most elementary form, “multi-modality imaging” connotes the evaluation of multiple image sets by a scientist or physician. Combining the information qualitatively from different imaging modalities such as X-ray, ultrasound and nuclear imaging has been an integral aspect of patient diagnosis and management in radiology since each modality was developed [4]. However, it has only been in the last two decades that advances in digital imaging hardware and software have allowed for the development of *quantitative* image synthesis whereby two (or more) *in vivo* imaging modalities are geometrically aligned and combined to provide clinical or scientific advantages over either of the two contributing modalities in isolation. For example, as the nuclear methods of PET and SPECT may lack clear anatomical landmarks, the co-registration of these data to modalities that depict high spatial resolution anatomical data is natural; in doing so the localization of radiotracer uptake measured by PET and SPECT is significantly improved [5]. The first hybrid SPECT-CT scanner was developed in 1989 [6,7], and the first PET-CT camera was reported in 2000 by Beyer *et al* [8]. Since that time, many studies have shown that SPECT-CT provides additional clinically useful information beyond either method on its own (see, e.g., [9-11]). Similarly, it has been noted that, “PET/CT is a more accurate test than either of its individual components and is probably also better than side-by-side viewing of images from both modalities” [12].

Given the success that PET-CT and SPECT-CT imaging have experienced, it is not surprising that considerable effort has been invested to develop hybrid PET-MRI devices [13,14]. The initial goal for integrating nuclear methods with CT (i.e., to provide information on anatomical landmarks) can also be provided by MRI. Indeed, for many relevant disease sites the anatomical information provided by MRI is superior to that provided by CT due to the greater inherent contrast resulting from differences in proton

density and the magnetic relaxation properties of tissue (to which MRI is sensitive) versus the differences in the electron density (to which CT is sensitive). Additionally, PET-CT is not without its limitations. These include radiation exposure associated with the CT component of the examination, artifacts due to CT-based attenuation correction (which are extrapolated from lower energy data) [15], motion in the time interval between the PET and CT acquisitions [16-18], and the not insignificant effects of iodine-based CT contrast agents on the quantification of PET data (summarized in [15]). Finally, MRI also offers a range of relevant, quantitative information on tumor biology related to, for example, blood flow, vascular and tissue spaces, pH and hypoxia, cellularity, and (*via* magnetic resonance spectroscopy) metabolite concentrations—all without exposing the patient to ionizing radiation. When these measurements are combined with those available from PET (e.g., glucose metabolism, cell proliferation, hypoxia, cell receptor expression), it is clear that these two modalities provide complementary information and create the opportunity to provide a more complete picture of a patient's cancer than either method on its own.

While it is possible to obtain sequential imaging data on stand-alone PET and MRI scanners and then fuse the images *via* retrospective image registration, such methods may be operator intensive and quite challenging, particularly for disease sites outside of the brain; that is, regions of the body that have deformable tissues (e.g., the breast) or undergo substantial changes during the hours or days separating the two scans (e.g., the intestinal tract). Furthermore, there can be significant changes in the underlying biology of interest during the between-scan time thereby fundamentally limiting several potential studies of interest. For example, for patient studies designed to look at early changes in response to a therapeutic intervention, it is imperative that there is no time delay between the two measurements – this is especially true for newer molecular targeted therapeutic agents, whose actions may occur in hours rather than days or weeks. Additional scientific investigations directed towards a range of studies, including the temporal correlation of changes in cell density (*via* diffusion weighted MRI, DW-MRI) and cell proliferation (*via* FLT-PET), or the distribution of a radiolabeled therapeutic in relation to underlying tumor blood flow, microvascular permeability and proliferation, are greatly facilitated through simultaneous acquisition, eliminating the potential confounds of changes in tumor status in space and time. Thus, as simultaneous PET-MRI allows for spatial and temporal co-registration of two modalities offering a wealth of complementary anatomical, physiological, and molecular information, the development of integrated PET-MRI devices has been undertaken in recent years.

The first publications reporting combined PET-MRI systems appeared in the mid to late 1990's, as groups from the University of California at Davis and King's College London [19-21], the University of Tubingen [22,23], and the University of Cambridge [24] all explored various approaches to integrating PET and MRI scanners. Shortly thereafter, exciting data in small-animal tumor studies began to emerge displaying the ability to simultaneously acquire quantitative PET and MRI data [14,25,26]. Today, integrated PET-MRI scanners are commercially available for clinical use, and several sites have begun to publish the first reports of their use in oncology [27,28]. These developments are particularly noteworthy because, in addition to providing exquisite soft-tissue contrast for identifying anatomical landmarks, MRI is capable of making quantitative measurements on a wide range of physiological, cellular, and molecular events that are of clinical utility. Thus, while PET-CT represents the integration of form (CT) and function (PET), PET-MRI offers the ability to integrate multiple functional readouts, which could have very important consequences for both clinical and research studies. However, it is not currently obvious where specifically such complex—and expensive— instrumentation will find practical clinical utility.

Here we highlight several of the key areas where simultaneously acquired PET-MRI measurements are anticipated to have a significant impact on clinical and/or research studies. By acquiring the data simultaneously, rather than sequentially, data from each modality can be temporally correlated and this facilitates several unique areas of investigation including MR-based motion corrections; the use of spatially and temporally co-registered anatomical MRI priors for improved reconstruction of PET data; improved arterial input function characterization for PET kinetic modeling; the development and use of dual-modality contrast agents; and patient comfort and practical convenience. We consider the relative advantages and disadvantages afforded by PET-MRI and summarize current opinions and evidence as to the likely value of PET-MRI in the diagnosis and management of cancer.

II. Towards improved quantification of PET data using MRI

Each positron emitted from a proton heavy nucleus may travel a short distance until it encounters an electron and annihilates to produce the two 511 keV photons (traveling approximately 180° apart) that are detected during PET image acquisition. Formation of an image in PET relies upon the coincidence detection of these two annihilation photons within a detector pair located on opposite sides of the subject being imaged. The line between the detector pair is termed the line of response (LOR), and millions of LORs are required in order to reconstruct a PET image. In general, anything causing errors in the number of coincidences measured for each LOR will result in degradation of the desired image. One major source of artifact is caused by the attenuation of the 511 keV photons before they reach the detectors. The overall probability of interaction between a 511 keV photon and tissue depends on the thickness and attenuation properties of the tissue the photon must traverse before reaching the detector, so the central portion of an object uniformly emitting positrons will appear to have a decreased concentration of the radionuclide source when compared to the periphery of the object. The process designed to address this issue in image reconstruction is called attenuation correction and methods based on theoretical considerations as well as direct measurements have both been proposed [29].

Early efforts at correcting attenuation were based on estimating the contour of the section of the body being imaged and assuming a uniform linear attenuation coefficient for that region of space. For example, in brain imaging, an ellipse would be “fit” to the contour of the skull as determined from the reconstructed emission data, and then a single linear attenuation coefficient would be assigned to the entire region and applied to correct the data for attenuation. A second reconstruction would then be carried out on the attenuation-corrected data. More advanced methods relied on segmenting various major structures from the emission sinogram (first introduced for brain imaging [30]) to determine regions of soft tissue and bone, though these approaches failed in non-homogeneous regions, resulting in overestimation of activity in regions adjacent to (for example) air cavities and thereby confounding interpretation of the resulting images. Consequently, methods that rely on transmission data have been developed.

Transmission scanning (reviewed in [31]) is based on positioning radioactive sources just inside the detector ring around the object to be imaged and collecting photons before (the so-called “blank scan”) and after the object is placed in the scanner, allowing the total attenuation along each LOR to be directly measured. While this technique increases the accuracy of attenuation correction, it introduces statistical noise (from limited photon counts due to limited source strength) and adds to total scan time. However, with the development of dedicated PET-CT scanners, the transmission scan has been essentially replaced by using CT data to directly assign the linear attenuation coefficient on a voxel-by-voxel basis. In this method, the Hounsfield units at the effective energy of the CT X-ray beam returned from the

CT reconstruction are converted to linear attenuation coefficients for 511 keV photons (a conversion for single energy CT studies not without its own assumptions) and then used to correct for attenuation of the emission photons. However, there is still the issue of mis-registration as the CT data are not acquired simultaneously with the PET data, and this fundamentally limits the accuracy a CT-based attenuation correction method can realize; errors of approximately 10% in the SUV have been reported [32,33]. Though retrospective (software-based) image registration can correct for such errors if the object in unchanging, hardware-based registration in which the images are acquired simultaneously and therefore inherently registered, something of greater importance for thoracic and abdominal imaging than (say) for the head. Simultaneous PET-MRI offers the potential to eliminate this specific problem.

There are, however, other concerns with the use of MRI for implementing accurate attenuation corrections. The signal intensity in standard MRI sequences are based on combinations of proton density and tissue relaxation properties—measurements that are not directly related to electron density and therefore not directly related to the linear attenuation coefficients of tissue. Using MRI measurements to correct for attenuation is not straightforward —though it is a rapidly developing field with several promising results published recently (see, e.g., [34-38]). Currently, the most investigated approach is to assign attenuation values based on tissue class assigned through segmentation of the MR image data. Segmentation of MR images is a maturing field, so there are several readily-applicable techniques available for this purpose (see, e.g., [39]). While soft tissues are typically easily segmented from MR images, the automatic differentiation of bone (with little to no proton signal when acquired using conventional MR methods) and air (no proton signal) is more complicated. To address this problem, some investigators have developed atlas-based methods which rely on multiple MR image sets that have been averaged to form a high SNR template to which attenuation coefficients are assigned to the various tissue regions [38,40]. Patient-specific attenuation correction is then performed by warping the new MRI data to the atlas followed by assigning the attenuation coefficients. Another potential approach for segmenting bone *via* MRI would be to employ so-called ultra-short echo time (UTE) imaging which enables the acquisition of data with echo times less than 100 μs, thereby allowing for the visualization of the very short T_2 of cortical bone [41].

A recent contribution compared the relative merits of segmentation- and atlas-based methods [38]. The segmentation approach was based on a whole-body Dixon fat-water segmentation [42] in which the MR images were partitioned into five tissue classes (not including bone) and each class was assigned an appropriate linear attenuation coefficient. The Atlas-based method employs a previously acquired database of aligned MRI-CT data sets that are then registered to the test data set in order to assign attenuation coefficients on a continuous scale. The two approaches were then compared in healthy as well as disease sites. In the healthy appearing tissues the average mean errors of the SUV were 14.1% and 7.7% for the segmentation- and atlas-based approaches, respectively. For the lesion sites, the errors were 7.5% and 5.7%, respectively. The authors concluded that the atlas-based approach was superior and this was due to the reduced errors made in areas near the bones and lungs.

A potential limitation of MR-based attenuation approaches is that methods developed for the head and brain are less likely to provide robust performance in whole-body MR imaging. First, despite continued improvements, there remain technical challenges for routinely obtaining high resolution, artifact-free MR images of the abdomen and chest. In this region, MR examinations tend to be targeted to specific studies where the improved contrast resolution of MR can solve specific diagnostic dilemmas, for example the evaluation of liver lesions, rather than as a routine tool for abdominal examinations, the province of CT.

Furthermore, there are significant challenges on the performance of segmentation algorithms and atlas based approaches below the neck, although there are ongoing efforts on this front [43-45]. As a result, improvements in the accuracy of attenuation correction in the abdomen are considered a work in progress.

Another challenge in attenuation correction in PET-MRI is to account for attenuation due to the RF coil (required for all MR acquisitions) which has been shown to adversely affect the quantitative accuracy of PET emission data by significant amounts [46]. As the coil does not appear in the MR image, its attenuation must be accounted for separately in an MR-based approach. One recent study provided evidence that a using a high-exposure CT to obtain a model of (in this particular case) a head coil could be used in a model-based correction that gave attenuation-corrected PET images that were comparable to the reference PET-CT reconstruction [47]. The authors noted that if there were errors in the positioning of the coil (on the order of a few millimeters), then artifacts emerged in the reconstructed PET image. Tellman *et al* found similar results on the importance of coil alignment [48]. Though challenging, careful engineering should adequately address this problem, as the geometry and composition of MR RF coils can be fixed for most, though not all, coil designs. Integration of PET/MR systems with advanced flexible coil designs, or endoscopic coils such as endorectal coils for prostate imaging, may require additional materials engineering work in reducing net attenuation of such designs, or real time feedback on their location.

Besides the use of MR data to correct for the effect of attenuation on PET data, simultaneously acquired MR images also offer the potential to improve PET images by providing anatomical information that can be incorporated into the PET image reconstruction process. Statistical reconstruction algorithms are replacing filtered backprojection as the method of choice for generating PET images from coincidence data, primarily because they provide a framework in which the physical properties of the data collection process can be modeled [49]. We expect different tissue types to exhibit different tracer uptake levels, so knowledge of tissue boundaries can be incorporated into the PET image reconstruction process to reduce blurring at those boundaries [50-52]. While these methods have been applied to PET-CT as well as retrospectively co-registered PET-MRI data, simultaneously acquired MRI data offers superior soft-tissue contrast with the most accurate spatial registration.

III. MRI-based motion correction of PET data

There are three major types of motion that must be considered during PET acquisition: gross motion (e.g., head movement or subtle patient repositioning due to discomfort), periodic movement (e.g., cardiac and respiratory motion), and internal shifting and distortion in the pelvic and abdominal regions (e.g., peristalsis). Motion during oncology applications can lead to errors in both lesion localization and quantification [53]. In the particular case of respiratory related motion, the practical image resolution can be degraded by a factor of five over the intrinsic resolution of the system [54]. Furthermore, motion causes blurring of tumors within the patient, making them appear larger in size while having a lower mean radiotracer uptake which, in turn, creates errors in quantification. By having the total activity distributed over a larger region of interest (ROI), the mean and maximum SUVs of the tumor will be underestimated. Additionally, such motion can entirely obscure the presence of smaller lesions. The problem is further exacerbated in dynamic imaging whereby any motion can potentially increase or decrease (in an unpredictable manner) the time activity course from a particular voxel resulting in decreased signal-to-noise and accuracy for estimating kinetic parameters.

Early methods of motion correction in PET relied on realigning individual frames to a reference position and then summing the result to obtain a single volume [55]. Others have explored the use of external tracking devices and video cameras to record when movements take place during image acquisition and using these time stamps to start new frames that could then be retrospectively registered [55]. Building on this approach, investigators have employed optical tracking systems combined with motion sensors placed on the periphery of the body. While this can be of value in dedicated brain imaging where corrections based on rigid transformations are sufficient to realign head motion, tracking the motion of the chest, for instance, provides limited information about internal non-rigid motion, such as how the diaphragm and heart move during the respiratory cycle. Additionally, visual tracking methods are often not applicable for PET-MR scanners as some RF coils preclude a clear view of the ROI being imaged.

It is important to note that CT-based methods for motion correction are limited by the fact that the CT and PET acquisitions do not occur simultaneously; that is, any motion occurring between the transmission and emission acquisitions will cause a spatial mismatch between the two data sets thereby compromising the integrity of the motion correction. As noted in section II, this mis-registration of the attenuation map will also adversely affect the quantitative accuracy and could give rise to artifacts.

Simultaneous PET-MRI potentially offers a practical, solution to the problem of correcting motion occurring during a PET acquisition. A natural way to make use of MR images to correct for PET motion is to simultaneously acquire high spatial resolution MR images while the PET data are being acquired. The MR images can then be retrospectively registered at the conclusion of data collection and the appropriate transformations can then be applied to the PET data. One recent study employing this approach was offered by Tsoumpas *et al* [54] in which standard gradient echo images were acquired with an in-plane resolution of 500 microns in 2.4 minutes while a dual-modality phantom was deformed in a controlled way. The MR data were used to correct for motion in the simultaneously acquired PET data, and corrected PET data were then compared with motion correction performed using only the PET data. While the MR-corrected approach yielded significantly better results, the authors also noted a number of limitations of the approach related to MR scan time and field of view.

Unfortunately, the acquisition of high spatial resolution MRI data (say, on the order of 1 mm^3 isotropic voxels) covering a moderately large FOV may take a few minutes to acquire and there can be motion during the acquisition of the MR images themselves, thereby limiting the effectiveness of such an approach (this limitation does not come into play in the acqusion of single shot echo planar imaging (EPI) or spiral images, such as are frequently used for diffusion or functional imaging). A more robust method, increasingly used in MR only acquisitions, is the use of one of a variety of real time navigation techniques. [see, e.g., 56,57]. These methods can assess subject position on time frames as short as the repetition time TR of the relevant MR acquisition - on order of one second. Data on the location of the object can then be used to adjust the LOR data prior to reconstruction.

A potentially exciting approach to extending MR-based motion correction of PET data to abdominal regions was recently contributed by Guerin *et al* [58]. Their approach made use of MRI tagging methods to track motion in order to estimate the deformation of tissue during the respiratory cycle. Tagged MRI allows estimation of the deformation of tissues by superimposing a regular tagging pattern on the object magnetization distribution. Guerin *et al* incorporated the (non-rigid) motion fields acquired from tagged MR images into an iterative PET reconstruction scheme. Simulations indicated that contrast estimation was 20% more accurate and that the SNR was 100% greater when the correction was incorporated.

The authors concluded that PET motion correction using motion fields derived from tagged-MRI is amenable to *in vivo* PET studies of the torso, though they acknowledge it is not yet applicable to correcting lung motion [58].

IV. Using MRI to inform PET kinetic modeling

There is an extensive literature on the use of compartmental modeling to understand the distribution and retention of various PET radiotracers (see, e.g., [59]). A series of ordinary, first-order, linear differential equations are often used to model the body as a series of well-mixed 'compartments' between which radiotracer may be transported. Solving the differential equations and then fitting those solutions to measured tissue time-activity curves (TACs) returns estimates of a number of relevant physiologic and biochemical parameters. Typical dynamic PET models return parameters describing the metabolic rates of tracer utilization. In order to perform accurate pharmacokinetic modeling of dynamic PET data, a number of measurements need to be obtained with high accuracy; in particular, the time course of the concentration of the radiotracer in a vessel feeding the ROI (the so-called arterial input function, or AIF) is required. Unfortunately, characterizing the AIF in a typical PET scan is challenging due to both the limited spatial resolution and the lack of available anatomical landmarks to define an arterial ROI.

The resolution of a PET scanner is mainly determined by the physical size and disposition of the radiation detectors. In clinical PET scanners, this resolution, as measured by the full-width at half maximum of the point spread function of the scanner, is approximately 4 to 5 mm [60,61]. This limited spatial resolution leads to the well-known partial volume effect (PVE), whereby the quantification of tracer uptake within a particular ROI is compromised by both activity spilling in from and out to adjacent tissues. The degree to which the PVE results in inaccuracy in estimating the concentration of tracer in a particular ROI depends on both the size of the ROI and the relative tracer activity between the ROI and the surrounding tissues [62,63]. For example, the PVE will lead to an overestimation of tracer uptake in an ROI surrounded by tissues with higher tracer uptake, and an underestimation when the ROI is surrounded by tissues with lower uptake values. In particular, it has been shown that PVE is negligible for regions with homogeneous uptake bigger than 2-3 times the spatial resolution of the scanner [62]. Thus, on most clinical scanners, quantification of ROIs smaller than 10-15 mm in any one dimension will be significantly affected by PVE. Given the small size of the vast majority of the arteries (< 10-15 mm) available within a typical field of view (FOV), the PVE represents a considerable barrier to accurate image-based AIF characterization.

The PET community has explored two main approaches to overcome the difficulty of characterizing the AIF for applications in oncology: obtaining blood samples from a peripheral vessel, and deriving the time course from the blood pool of the left ventricle. For the former, arterial samples are taken at regular time intervals (defined according to the needs and specifications of the pharmacokinetics of the radiotracer) and radioactivity is determined in a gamma well counter to derive the radiotracer concentration in the blood at the time of sampling. This approach has the obvious advantage of being able to provide very accurate quantification of the AIF (see, e.g., [64,65]). For applications in which the heart is contained within the FOV, the AIF can be estimated by placing an ROI inside the left ventricle which is sufficiently large to minimize the PVE. However, these two common solutions suffer from fundamental limitations. For example, blood sampling is obviously (minimally) invasive and impractical in many clinical settings. Additionally, the concentration of the tracer is known only from a peripheral vessel which may have a very different AIF shape, due to delay and dispersion, from that in a vessel feeding the ROI. Obtaining the AIF from the left ventricle also may not be practical if the heart is not within

the FOV or if the radiotracer being used exhibits uptake in the myocardium. Furthermore, the heart is continuously in motion which can lead to errors in ROI placement and subsequent AIF estimation. More reliable and clinically relevant alternatives would have high practical impact.

Simultaneous PET-MRI enables the acquisition of inherently spatially and temporally registered PET and MR images, so it may offer solutions to the problems related to spatial resolution listed above. MRI enables accurate delineation and differentiation of the lumen from the wall of the vascular bed. Figure 1 presents an example of an inflamed arterial wall in the left common carotid that if segmented improperly would lead to an overestimation of the AIF which would, subsequently, result in errors in the parameters returned from kinetic modeling. Figure 2 shows another example where time-of-flight MR clearly identifies the arterial blood pool; this sequence is of particular use in areas where arteries are extremely narrow and segmentation is challenging, as is frequently the case for brain studies (Fig. 2b).

In addition to enhancing the reliability of segmenting tissue to obtain an accurate AIF, the addition of MRI to a dynamic PET study can also assist in correction of the PVE. Partial volume correction (PVC) methods have focused on refining the accuracy of quantification of tracer concentration [66-69]. The geometric transfer matrix MR-based method, first described by Rousset *et al.* [67], describes and corrects for the regional interactions between adjacent tissues. Previous implementations of this method were limited by the need to accurately co-register MR and PET data, as well as the requirement to segment homogeneous uptake regions. Simultaneous PET-MRI offers for the first time inherently co-registered PET and MR data wherein the high-resolution anatomical MRI data can provide highly accurate segmentation of tissues to reduce errors in manual segmentation of the PET data, thereby optimizing the PVC algorithm (see discussions in sections II and III above).

A second PVC technique that relies on spatially and temporally registered PET-MRI data is designed to increase contrast in PET images in order to, for example, improve the ability to delineate volumes of interest from surrounding tissues [68]. The method is based on performing a multi-resolution analysis to integrate high-resolution data, H, (e.g., from anatomical MR images) into a lower resolution PET image, L. The wavelet transform is then used to obtain the spatial frequencies at each level of resolution that is common to both H and L. Then a model is used to build the missing high-frequency data in L from H. Studies have shown that the approach enhances contrast and improves the ability to delineate boundaries [69]. Using this approach, simultaneous PET-MRI would not only provide co-registered PET and MR images, but also enable the improvement of PET spatial resolution and contrast. Recent efforts have combined the technique with anatomical probabilistic atlases to yield PVE-corrected functional volumes of great accuracy, and the results have begun to be deployed in clinical studies [70].

The topics discussed above in sections II and III can also assist in improving the accuracy of quantitative PET by reducing motion error (and the associated increase in noise) and improving PET reconstruction *via* anatomical priors. MR could be used for detecting and tracking motion due to respiration, the cardiac cycle, and gross patient movement during the dynamic PET acquisition. Of course, by improving the PET reconstruction using the anatomical priors available from the MRI data, the PVE is reduced.

V. Development of dual-modality contrast agents

A fundamental question surrounding the potential future use and clinical application of dual PET-MRI contrast agents is the vast difference in inherent sensitivities of the two techniques; PET studies require picomolar concentrations of the tracer, while the typical gadolinium MRI contrast agents require millimolar concentrations. However, this issues

have not deterred the field from developing agents that can be detected simultaneously by each modality. To partially span the sensitivity gap, agents have been developed by tethering positron emitters to dextran coated superparamagnetic iron oxide (SPIO) nanoparticles which require only micromolar concentrations to achieve reasonable MR contrast. We now briefly highlight some recent illustrative examples of this approach.

Torres *et al* attached ^{64}Cu to a bisphosphonate (bp) group that binds to the dextran surface [71] of a SPIO. The copper is chelated within dithiocarbamate (dtc) to form [^{64}Cu(dtcbp)^{2}] which has great affinity for the SPIO's dextran. Upon *in vivo* (sequential) PET-MRI imaging, this construct showed retention only in the popliteal and iliac lymph nodes. Another example of a ^{64}Cu-MION probe was developed by Glaus *et al* who coated an SPIO with polyehtylene glycol (PEG) phospholipids. DOTA (1,4,7,10-tetraazacyclo-dodecane-1,4,7,10-tetraacetic acid) was used to chelate ^{64}Cu and then conjugated to the PEG [72]. The authors performed *in vivo* pharmacokinetic analysis with their construct in a murine model *via* microPET/CT and organ biodistribution studies. They concluded that the ability of the agent to have high initial blood retention with only moderate liver uptake makes it a potentially attractive contrast agent. They also noted that, in general, linking the PET agent to the nanoparticle provides improved circulation half-life [72].

Noting that the lymphatic system is a common route of metastases for cancer, Choi *et al* designed an agent to selectively image sentinel lymph nodes [73]. In constructing their PET-MRI tracer, the investigators began with $MnFe_2O_4$ and coated the surface with cross-linked serum albumin for stabilization resulting in a 32 nm probe appropriate for lymphatic imaging. The PET radionuclide ^{124}I can then be directly conjugated to the tyrosine residue on the serum albumin to generate a dual-modality probe. The authors present *in vivo* data in a rat model showing both MR and PET localization of probe within the brachial and axillary lymph nodes.

An example of a cell-surface targeted PET-MRI probe was developed and applied *in vivo* by Lee *et al* [74]. Polyaspartic acid (PASP)-coated iron oxide (PASP-IO) nanoparticles were synthesized and the surface amino groups were coupled to the arginine-glycine-aspartic peptide sequence for active targeting to the $\alpha_v\beta_3$ integrin. (The integrins are known to play a fundamental role in angiogenesis and many groups have developed tracers and contrast agents to specifically image them, particularly, $\alpha_v\beta_3$, in order to assess their expression [75].) DOTA was again used to chelate ^{64}Cu. The *in vivo* data showed that the investigators were able to achieve specific targeting (though some nonspecific accumulation was observed) of the receptor in mice bearing U87MG tumors.

A final dual-modality example to consider is the probe developed by Frullano *et al* [76]. They noted that a PET-MRI agent could potentially allow for quantification of both concentration and relaxivity which would enable a host of possible applications, including quantitative pH imaging. In these initial studies, simultaneous PET-MRI measurements were acquired in phantoms with known pH and the PET signal was used to determine the absolute concentration of the tracer, which was then combined with MR relaxation measurements to determine the pH of the phantoms. The authors showed good correspondence between the pH measured by an electrode and that calculated from imaging data.

The last example is particularly important because it simplifies the measurement of pH which is difficult by using just one of the modalities. Another, similar, utility for a dual PET-MRI tracer would be to remove the ambiguity inherent in pharmacokinetic modeling of contrast-enhanced MRI studies. As the contrast agent is not directly measured in an MRI experiment (its presence is merely inferred based on its effect on relaxation times), its concentration is difficult to quantify absolutely. This fact limits the ability to perform

quantitative modeling in, for example, dynamic (T_1-weighted) contrast-enhanced MRI studies or in dynamic (T_2-weighted) susceptibility contrast MRI studies. However, the counts registered in a PET study are directly proportional to the concentration of tracer present in the voxel or region of interest (ROI), so quantification of tracer concentration is straightforward in PET. Thus, one could potentially use PET to determine the time course of the concentration of the tracer (through appropriate calibration) in the ROI and use this knowledge to inform DCE- or DSC-MRI pharmacokinetic modeling. However, the issue of divergent sensitivities of the two modalities remains. Frullano *et al.* [76] addressed this problem by producing a low specific activity PET-MR agent so that a sufficient concentration of the MR component could be achieved while maintaining an appropriate amount of injected radioactivity. However, given the limited sensitivity of MRI, PET-MR probes, in general, cannot be considered “tracers” in the traditional sense which may limit the potential targets for such dual-modality agents.

Beyond such examples it is not immediately clear how many dual PET-MRI tracers present advantages over a corresponding single modality tracer. Several of the above referenced papers commented on the potential for improved diagnostics (in terms of increased sensitivity and specificity) and greater understanding of the underlying biology, but it is not self-evident that this should be the case. Currently, there is a paucity of data demonstrating the value in localizing a dual-modality tracer beyond merely the ability to detect it with both modalities (particularly, given the exquisite molecular sensitivity of PET); that is, what new information can be learned by simultaneously detecting the agent by both modalities? As discussed in the next section, however, contrast agent “cocktails” (injections of two agents: one for PET and one for MRI) is of potential interest.

VI. Possible clinical applications of PET-MRI in oncology

It is instructive to divide the potential uses of PET-MRI in oncology into short- and long-term applications. Short-term applications include those that would require minimal new studies or validation in order to implement PET-MRI in clinical practice. Long-term applications are those which logically stand to benefit from the spatial and temporal co-registration of PET and MRI functional measures, but for which there is currently a paucity of supporting data.

Potential short-term applications of PET-MRI in oncology include both disease staging and clinical situations calling for detailed characterization of a particular lesion or region. For disease staging, combined PET-MRI may offer advantages over separate PET and MRI examinations for measuring the distribution of disease over the whole body, while simultaneously providing required high spatial resolution imaging of one particular disease site; that is, PET can provide whole-body assessment thereby guiding selection of a limited FOV for subsequent MRI and/or MR spectroscopy (MRS) measurements. Examples from current oncology practice include whole-body staging of lymphoma or melanoma with simultaneous high spatial resolution evaluation of known brain metastases, or whole-body staging of breast cancer with simultaneous high spatial resolution imaging of the breast for surgical planning. In other staging situations there may be a compelling reason to use PET-MRI over PET-CT, e.g., in the presence of an iodine allergy or in pediatric populations where patients may face repeated imaging sessions and there is strong motivation to minimize radiation exposure.

For detailed characterization of a particular lesion, there is emerging evidence of synergistic value of simultaneous PET and MRI for certain indications, including local staging, treatment planning, and response assessment. Recent studies have described such potential synergies for brain, head/neck, and pancreatic malignancies. For brain tumor radiation

treatment planning, one recent study showed advantages of adding ^{18}F-fluoro-ethyl-tyrosine to anatomical MRI for determining the gross tumor volume (GTV) for high-grade glioma [77]. A similar result was found in a meningioma case study in which ^{68}Ga-DOTATOC was employed during simultaneous PET-MRI [78]. The authors used both the PET and MRI data to delineate the GTV and concluded that the combination of the two techniques is clinically feasible, allowed a more detailed visualization of the tumor, may be more accurate for delineation of the target volume, and may improve the workflow for radiation therapy planning. While both of these studies made use of simultaneous PET-MRI, there have also been studies that have employed retrospective PET-MRI registration to assess the ability of the two modalities to improve patient care.

For head and neck cancer, Huang *et al.* investigated the diagnostic value of FDG-PET co-registered to anatomical MRI compared to PET-CT, CT, and MRI in advanced buccal squamous cell carcinoma (BSCC; [79]). The authors found that fused PET-MRI images have the highest sensitivity and specificity of the four approaches. Furthermore, tumor size (i.e., mean maximal diameter) as measured by PET-MRI had a higher correlation coefficient (r^2=0.96) with pathologic tumor size than CT (r^2=0.55), MRI (r^2=0.58), or PET/CT (r^2=0.74). The authors concluded that fused PET-MRI is more reliable for assessment of invasion and tumor size delineation in advanced BSCC [79].

For pancreatic cancer, Tatsumi *et al.* recently contributed a study in which they retrospectively registered 47 FDG-PET data sets to anatomical MRI in order to demonstrate the feasibility of PET-MRI to evaluate pancreatic cancer [80]. They assessed the ability of PET-MRI to visualize the tumors using a five-point scale and also assessed the overall image quality using a three-point scale, with all evaluations compared to PET-CT. The fused PET-MRI data were able to offer additional diagnostic information over stand-alone PET, and the overall image quality was higher with PET-MRI. While not statistically significant, the diagnostic accuracy of PET-MRI was higher (93.0%) than PET-CT (88.4%). This study is of particular interest because it involves image registration of a disease site that is below the neck, where retrospective image registration is especially challenging due to a paucity of rigid fiducials as well as the presence of peristaltic motion.

These preliminary studies likely represent a small sample of potential synergies when combining PET and MRI for characterization of specific lesions. Other possible short-term indications for PET-MRI include characterization of suspected bone or soft tissue sarcomas, evaluation of tumor recurrence at surgical resection sites, and a variety of *ad hoc* "problem solving" situations where one might expect enhanced diagnostic accuracy from co-registered functional information and high-resolution anatomic detail. However, it should be noted that although hybrid imaging appeared to improve technical metrics and the confidence of the oncologist and radiologist, none of these studies represent a critical evaluation of outcome. While all involved believe that striving to improve image quality and the level of information achieved is advantageous, it remains to be proven whether this also translates into improved patient outcomes or reduced morbidity.

Addressing the long-term implications of simultaneous PET-MRI in oncology is necessarily more speculative as it relies on "emerging" or "future" applications requiring rigorous spatial and temporal co-registration of PET and MRI physiological, cellular, and molecular data. As noted above, there are currently few examples exploring such data sets. However, an illustrative example may help to elucidate some possible avenues to investigate in future studies. Figure 3 displays a multi-parametric approach to monitoring an invasive ductal carcinoma during neoadjuvant chemotherapy (NAC). Specifically, quantitative DCE- and DW-MRI parameters have been registered to an FDG-PET scan at three time points during NAC: 1) pre-therapy (column 1), 2) after one cycle of therapy (column 2), and 3) at the

conclusion of NAC but prior to surgery (column 3). Each row presents a quantitative parameter map at each time point. The first three rows present data available from a DCE-MRI study: row 1 displays the volume transfer constant (K^{trans}, reporting on vessel perfusion-permeability), row 2 displays the extravascular extracellular volume fraction (v_e), and row 3 displays the plasma volume fraction (v_p). Also available from the MRI study is an apparent diffusion coefficient (ADC, row 4) map reporting on tumor cellularity. The final row presents the FDG-PET map at each time point. Clearly, there is a wealth of important, clinically relevant information in these data and, while there is a developing literature on the ability of DCE-MRI, DW-MRI, and FDG-PET to monitor and/or predict therapy response, there is currently a paucity of data that have synthesized such measurements. Going forward, integration of quantitative PET and MRI metrics offers the promise of enhancing both clinical and basic cancer biology studies.

The first, and perhaps most obvious, avenue is to test the hypothesis that “more data” will yield more sensitive and specific diagnostic information. By longitudinally tracking the temporal relationship between parameters, or combinations thereof, one can learn which parameters are most sensitive the effects of various therapies. In fact, there are exciting initial studies available for using retrospectively registered PET-MRI data to diagnose breast lesions [81]. (Note: here we use “retrospective” in the sense of using separate PET and MRI scanners and performing the registration off-line.) Moy *et al.* found that when the (clinical) DCE-MRI and (prone) FDG-PET data were combined, there were marked improvements in several of the standard diagnostic statistics. For example, the sensitivity was 83% (up from 57% for PET alone), specificity was 97% (up from 53% for MRI alone), the positive predictive value was 98% (up from 77% for MRI alone), and the negative predictive value was 80% (up from 59% for PET alone). Furthermore, the false-negative rate was reduced to 9% (down from 27% for PET alone). In light of these results, it is not an unreasonable hypothesis that combined PET-MRI will facilitate more accurate and precise monitoring and prediction of response in the therapeutic setting.

Collecting quantitative, multi-modal, multi-parametric data also presents the opportunity to perform basic cancer biology studies. For example, studying how the individual parameters change spatially and temporally could enable the formation of hypotheses related to how individual pharmaceuticals work in vivo. The different measurements report on different aspects of the same treatment, so it may be possible to visualize (noninvasively) the various downstream effects (i.e., drug activity) of a given therapeutic regimen. Furthermore, it may be possible to form hypotheses on an individual basis thereby contributing to personalized medicine in a very practical manner.

There is also the ability to develop fundamental imaging science. By studying how the quantitative parameters change spatially and temporally, it may be possible to learn more about the appropriate interpretation of the parameters themselves by cross-validation and visualization. For example, simple correlation analysis of various parameters may provide insights into their relationship which can subsequently be used to more comprehensively characterize the tissue giving rise to those measures. For example, by combining measurements of DW-MRI and ^{18}F-fluodeoxythymidine PET, it may be able possible to determine the overall proliferative capacity for a given section of tissue. By synthesizing data from DCE-MRI and ^{18}F-fluoromisonidazole PET, we may be able to elucidate the temporal and spatial relationship between angiogenesis and hypoxia *in vivo*. While there are some initial studies that have been contributed in the literature [82-84], this is currently an underexplored area of research. Finally, spatially and temporally integrated PET-MRI data present the opportunity to perform practical—clinically relevant— imaging-guided mathematical modeling of tumor growth [85].

VII. Patient comfort and convenience

An integrated PET-MRI scanner can have a very real and beneficial effect on patient comfort and convenience. Currently, if a research or clinical study requires both PET and MRI data, the patient must endure two exams in confining scanners which is problematic for patients who suffer from even mild claustrophobia. This duplication not only increases the discomfort (both physical and psychological) the patient must endure, but also effectively doubles the chances of motion during one or both scans with the subsequent need to re-scan particular sequences or even the entire study. In light of the discussion in the previous section if, as some studies suggest, there is an added diagnostic benefit to combing PET and MRI, then it is of great import to minimize the difficulties associated with acquiring both data sets. The problem of patient anxiety and discomfort is a well-known phenomenon extending back (at least) to the first few years after the widespread introduction of clinical MRI [86-89]. A review of the topic shows that as many as 37% (range: 4%-37%) of patients undergoing MRI had an anxiety-related reaction to the procedure [90,91]. In one study, which found that approximately 14% of MRI patients required some form of sedation to tolerate a standard-of-care MRI, the use of sedation was actually more common in patients who had already had previous MRI exams, indicating that familiarity with the procedure may not reduce stress related to the procedure [92].

The problem of anxiety and discomfort during imaging is not unique to MRI, as similar issues arise for PET examinations. It has been noted that a patient that is stressed and fidgeting can have elevated FDG uptake in skeletal muscle, which may adversely affect tumor-to-muscle ratio measurements [93]. Additionally, there is a well-known anxiety-induced increase in FDG uptake in brown fat that has been linked to false-positive interpretations in 2-4% of all studies, as well as false-negatives due to brown fat uptake masking lesion detectability [94-96]. The problem is often exacerbated in pediatric patients where stress-induced muscle tension, crying and the associated coughing can yield increased muscle FDG uptake [97]; these issues are well-known amongst technologists and efforts have been made to address the particular issues surrounding pediatric PET studies [98].

A final, extremely practical, point to note is that a combined PET-MRI exam would preclude the patient from having to endure the (sometimes lengthy) periods in multiple waiting rooms waiting for their scans. As many of these patients are missing work and/or traveling from far distances to undergo their testing, a combined exam would undoubtedly enhance their experience and make it more tolerable. For the cancer patient who already may not have a great deal of strength to attend these imaging tests, eliminating one set of waiting rooms and preps would be greatly appreciated.

The above data underscore the importance of considering patient comfort and convenience in order to eliminate as many obstacles as possible to accurate, reproducible measurements of contrast agents (MRI) and tracer uptake (PET) which are a requirement in assessing, for example, treatment response over longitudinal studies. A truly simultaneous PET-MRI acquisition would effectively reduce total scan time by 50%, thereby reducing patient anxiety, increasing patient comfort, decreasing repeat scanning and callbacks, and potentially increasing scanner throughput. Additionally, the elimination of CT for anatomical landmarks results in a significant reduction in radiation dose to the patient. Simultaneous PET-MRI is likely to positively affect the imaging experience, at least for critical patient populations.

VIII. Summary

Our understanding of cancer has evolved to the point that many tumors are no longer simply treated according to their organ site; that is, they are defined according to particular genetic

and molecular markers. Consequently, as drugs become more specific to target those unique markers, the broad sword that is morphological imaging (see, e.g., the response evaluation criteria in solid tumors, RECIST [99]) will not be appropriate for assessing—let alone predicting—therapy response. This is a fact not lost on the imaging community as there has been an explosion of quantitative imaging metrics and targeted radiopharmaceuticals in recent years. Unfortunately, while there has been a steady increase in both the quality and quantity of quantitative imaging metrics that can report on tumor status, these methods have not been moved effectively to routine clinical use. Nor have data from different techniques been effectively integrated to provide a comprehensive assessment of tumor status. This is partly due to the fact that it is currently very difficult to perform multi-parametric, multi-modality studies in the clinical setting. The development of simultaneous PET-MRI provides an opportunity to address these issues and potentially accelerate the validation and adoption of emerging imaging biomarkers into clinical trials and practice.

For widespread acceptance, a compelling case could arise if the combination of quantitative MRI and specific PET biomarkers significantly improves our ability to assess tumor state and response to therapy, and some likely candidates are now evolving. As discussed above, the simultaneous acquisition of MRI data can be used as *a priori* knowledge to both improve the accuracy of the reconstructed PET images, as well as minimize the artifacts due to motion. MRI data can also be used to inform PET kinetic modeling by, for example, reducing partial volume errors and assisting with AIF characterization. In addition to technical developments such as these, simultaneous PET-MRI may increase patient comfort and convenience as clinical situations that call for two separate scanning sessions (and the associated hassles of two waiting rooms, longer time away from work or home, etc.) will be reduced to one. Of course, simultaneous PET-MRI is not without its limitations. For example, attenuation correction and whole-body imaging by MR are still technically challenging and further investigation will be required to establish practical, clinically relevant, solutions. Moreover, the development of true dual-modality contrast agents will require significant investment, not the least due to the challenges of getting new diagnostic imaging agents approved in the current regulatory climate, especially those needing administration in the millimole/kg range. Finally, the rather large price tag associated with today's devices may prove prohibitive for many institutions.

Perhaps the most exciting opportunity for simultaneous PET-MRI is the ability to combine multi-parametric data to address a myriad of clinical and basic science questions. As Figure 3 indicates, there is a wealth of information in these data sets and it is hard to believe that, if such data sets could be acquired routinely, that we would not be able to increase our: 1) sensitivity and specificity of diagnoses, 2) ability to stratify patients into different therapeutic options, 3) ability to assess (even predict) response early in a therapeutic regimen, and 4) ability to identify recurrent disease earlier than current methods. Furthermore, such data could be integrated with other available clinical data to obtain a more comprehensive picture of tumor status, thereby hastening the arrival of personalized medicine. Beyond these very important clinical questions, we can potentially use such data sets to learn, noninvasively, about mechanisms of drug effects. In order to achieve these goals, we will need to develop (and in some cases, invent) methods for intelligent statistical and mathematical modeling of multi-parameter imaging data that has both spatial and temporal dimensions. Such approaches are currently being investigated in the pre-clinical setting where there has been a tremendous growth of basic and applied PET-MRI studies. As these methods mature, investigators will naturally want to push them into clinical application, thereby providing another driving force for the eventual clinical acceptance of simultaneous PET-MRI.

In summary, just as integrating PET-CT and SPECT-CT yielded clinically relevant information superior to either modality on its own, simultaneous PET-MRI may do the same for many disease sites and situations.

Acknowledgments

T.E.Y., T.E.P, H.C.M., L.R.A., X.L., N.C.A., and J.C.G. thank the National Institutes of Health for support through NCI U01 CA142565, NCI R01CA138599, NCI 1P50 CA098131, NCI P30 CA68485, NCI 1R01 CA140628, NCI K25 CA127349, NCI 1RC1 CA145138. Additionally, we thank the Kleberg Foundation for generous support of the molecular imaging program at Vanderbilt University. D.I.G. and Z.A.F. thank the NIH for support through NHLBI R01 HL071021 and R01 HL078667. C.C. and B.R. thank the NIH for support through NCI 1 R01 CA137254-01A1 and NCI U01CA154601-01. We thank Dr. Bruce Rosen, M.D., Ph.D. for reviewing and editing an early version of the manuscript.

References

1. Afaq A, Akin O. Imaging assessment of tumor response: past, present and future. Future Oncol. 2011; 7(5):669–77. [PubMed: 21568682]
2. Schnall M, Rosen M. Primer on Imaging Technologies for Cancer. J Clin Oncol. 2006; 24:3225–33. [PubMed: 16829646]
3. Levin CS. Primer on molecular imaging technology. Eur J Nucl Med Mol Imaging. 2005; 32:S325–S345. [PubMed: 16341514]
4. Webb, S. Physics of Medical Imaging. Institute of Physics Publishing; London: 1988.
5. Correia JA. Editorial: Registration of Nuclear Medicine Images. J Nucl Med. 1990; 31:1227–9. [PubMed: 2362202]
6. Hasegawa BH, Gingold EL, Reilly SM, et al. Description of a simultaneous emission-transmission CT system. In Medical Imaging IV: Image Formation. Proc SPIE. 1990; 1231:50–60.
7. Hasegawa BH, Iwata K, Wong KH, Wu MC, Da Silva AJ, Tang HR, Barber WC, Hwang AH, Sakdinawat AE. Dual-modality imaging of function and physiology. Acad Radiol. 2002; 9(11): 1305–21. [PubMed: 12449363]
8. Beyer T, Townsend DW, Brun T, et al. A combined PET/CT scanner for clinical oncology. J Nucl Med. 2000; 41:1369–1379. [PubMed: 10945530]
9. Horger M, Bares R. The role of single-photon emission computed tomography/computed tomography in benign and malignant bone disease. Semin Nucl Med. 2006; 36(4):286–94. [PubMed: 16950146]
10. Even-Sapir E, Keidar Z, Sachs J, Engel A, Bettman L, Gaitini D, Guralnik L, Werbin N, Iosilevsky G, Israel O. The new technology of combined transmission and emission tomography in evaluation of endocrine neoplasms. J Nucl Med. 2001; 42(7):998–1004. [PubMed: 11438618]
11. Pfannenberg AC, Eschmann SM, Horger M, Lamberts R, Vonthein R, Claussen CD, Bares R. Benefit of anatomical-functional image fusion in the diagnostic work-up of neuroendocrine neoplasms. Eur J Nucl Med Mol Imaging. 2003; 30(6):835–43. [PubMed: 12682789]
12. von Schulthess GK, Steinert HC, Hany TF. Integrated PET/CT: Current Applications and Future Directions. Radiology. 2006; 238:405–22. [PubMed: 16436809]
13. Catana C, Procissi D, Wu Y, Judenhofer MS, Qi J, Pichler BJ, Jacobs RE, Cherry SR. Simultaneous in vivo positron emission tomography and magnetic resonance imaging. Proc Natl Acad Sci U S A. 2008; 105(10):3705–10. [PubMed: 18319342]
14. Judenhofer MS, Wehrl HF, Newport DF, Catana C, Siegel SB, Becker M, Thielscher A, Kneilling M, Lichy MP, Eichner M, Klingel K, Reischl G, Widmaier S, Röcken M, Nutt RE, Machulla HJ, Uludag K, Cherry SR, Claussen CD, Pichler BJ. Simultaneous PET-MRI: a new approach for functional and morphological imaging. Nat Med. 2008; 14(4):459–65. [PubMed: 18376410]
15. Mawlawi O, Pan T, Macapinlac HA. PET/CT imaging techniques, considerations, and artifacts. J Thorac Imaging. 2006; 21(2):99–110. [PubMed: 16770227]
16. Osman MM, Cohade C, Nakamoto Y, et al. Respiratory motion artifacts on PET emission images obtained using CT attenuation correction on PET-CT. Eur J Nucl Med Mol Imaging. 2003; 30:603–606. [PubMed: 12536242]

17. Goerres GW, Kamel E, Heidelberg TN, et al. PET-CT image coregistration in the thorax: influence of respiration. Eur J Nucl Med Mol Imaging. 2002; 29:351–360. [PubMed: 12002710]
18. Beyer T, Antoch G, Blodgett T, et al. Dual-modality PET/CT imaging: the effect of respiratory motion on combined image quality in clinical oncology. Eur J Nucl Med Mol Imaging. 2003; 30:588–596. [PubMed: 12582813]
19. Shao Y, Cherry SR, Farahani K, Meadors K, Siegel S, et al. Simultaneous PET and MR imaging. Phys. Med. Biol. 1997; 42:1965–70. [PubMed: 9364592]
20. Shao Y, Cherry SR, Farahani K, Slates R, Silverman RW, et al. Development of a PET detector system compatible with MRI/NMR systems. IEEE Trans. Nucl. Sci. 1997; 44:1167–71.
21. Slates RB, Farahani K, Shao Y, Marsden PK, Taylor J, et al. A study of artefacts in simultaneous PET and MR imaging using a prototype MR compatible PET scanner. Phys. Med. Biol. 1999; 44:2015–27. [PubMed: 10473211]
22. Pichler BJ, Wehrl HF, Kolb A, Judenhofer MS. Positron emission tomography/magnetic resonance imaging: the next generation of multimodality imaging? Semin Nucl Med. 2008; 38(3):199–208. [PubMed: 18396179]
23. Pichler BJ, Wehrl HF, Judenhofer MS. Latest advances in molecular imaging instrumentation. J Nucl Med. 2008; 49(Suppl 2):5S–23S. [PubMed: 18523063]
24. Lucas AJ, Hawkes RC, Ansorge RE, Williams GB, Nutt RE, Clark JC, Fryer TD, Carpenter TA. Development of a combined microPET-MR system. Technol Cancer Res Treat. 2006; 5(4):337–341. [PubMed: 16866564]
25. Pichler BJ, Judenhofer MS, Catana C, Walton JH, Kneilling M, Nutt RE, Siegel SB, Claussen CD, Cherry SR. Performance test of an LSO-APD detector in a 7-T MRI scanner for simultaneous PET/MRI. J Nucl Med. 2006; 47(4):639–47. [PubMed: 16595498]
26. Maramraju SH, Smith SD, Junnarkar SS, Schulz D, Stoll S, Ravindranath B, Purschke ML, Rescia S, Southekal S, Pratte JF, Vaska P, Woody CL, Schlyer DJ. Small animal simultaneous PET/MRI: initial experiences in a 9.4 T microMRI. Phys Med Biol. 2011; 56(8):2459–80. [PubMed: 21441651]
27. Boss A, Bisdas S, Kolb A, Hofmann M, Ernemann U, Claussen CD, Pfannenberg C, Pichler BJ, Reimold M, Stegger L. Hybrid PET/MRI of intracranial masses: initial experiences and comparison to PET/CT. J Nucl Med. 2010; 51(8):1198–205. [PubMed: 20660388]
28. Boss A, Stegger L, Bisdas S, Kolb A, Schwenzer N, Pfister M, Claussen CD, Pichler BJ, Pfannenberg C. Feasibility of simultaneous PET/MR imaging in the head and upper neck area. Eur Radiol. 2011; 21(7):1439–46. [PubMed: 21308378]
29. Cherry, SR.; Dahlbom, M. PET: Physics, instrumentation, and scanners. In: Phelps, ME., editor. PET Molecular Imaging and its Biological Applications. Springer; New York: 2004. p. 1-124.
30. Bergström M, Litton J, Eriksson L, Bohm C, Blomqvist G. Determination of object contour from projections for attenuation correction in cranial positron emission tomography. J Comput Assist Tomogr. 1982; 6(2):365–72. [PubMed: 6978896]
31. Bailey DL. Transmission scanning in emission tomography. Eur J Nucl Med. 1998; 25(7):774–87. [PubMed: 9662601]
32. Visvikis D, Costa DC, Croasdale I, Lonn AH, Bomanji J, Gacinovic S, et al. CT-based attenuation correction in the calculation of semi-quantitative indices of [18F]FDG uptake in PET. Eur J Nucl Med Mol Imaging. 2003; 30:344–53. [PubMed: 12634961]
33. Westerterp M, Pruim J, Oyen W, Hoekstra O, Paans A, Visser E, et al. Quantification of FDG PET studies using standardised uptake values in multi-centre trials: effects of image reconstruction, resolution and ROI definition parameters. Eur J Nucl Med Mol Imaging. 2007; 34:392–404. [PubMed: 17033848]
34. Keereman V, Holen RV, Mollet P, Vandenberghe S. The effect of errors in segmented attenuation maps on PET quantification. Med Phys. 2011; 38(11):6010–9. [PubMed: 22047365]
35. Catana C, van der Kouwe A, Benner T, Michel CJ, Hamm M, Fenchel M, Fischl B, Rosen B, Schmand M, Sorensen AG. Toward implementing an MRI-based PET attenuation-correction method for neurologic studies on the MR-PET brain prototype. J Nucl Med. 2010; 51(9):1431–8. [PubMed: 20810759]

36. Marshall HR, Stodilka RZ, Theberge J, Sabondjian E, Legros A, Deans L, Sykes JM, Thompson RT, Prato FS. A comparison of MR-based attenuation correction in PET versus SPECT. Phys Med Biol. Jul 21; 2011 56(14):4613–29. [PubMed: 21725141]
37. Malone IB, Ansorge RE, Williams GB, Nestor PJ, Carpenter TA, Fryer TD. Attenuation correction methods suitable for brain imaging with a PET/MRI scanner: a comparison of tissue atlas and template attenuation map approaches. J Nucl Med. Jul; 2011 52(7):1142–9. [PubMed: 21724984]
38. Hofmann M, Bezrukov I, Mantlik F, Aschoff P, Steinke F, Beyer T, Pichler BJ, Schölkopf B. MRI-based attenuation correction for whole-body PET/MRI: quantitative evaluation of segmentation- and atlas-based methods. J Nucl Med. 2011; 52(9):1392–9. [PubMed: 21828115]
39. Zaidi H, Montandon ML, Slosman DO. Magnetic resonance imaging-guided attenuation and scatter corrections in three-dimensional brain positron emission tomography. Med Phys. 2003; 30(5):937–48. [PubMed: 12773003]
40. Salomon A, Goedicke A, Schweizer B, Aach T, Schulz V. Simultaneous reconstruction of activity and attenuation for PET/MR. IEEE Trans Med Imaging. 2011; 30(3):804–13. [PubMed: 21118768]
41. Robson MD, Gatehouse PD, Bydder M, Bydder GM. Magnetic resonance: an introduction to ultrashort TE (UTE) imaging. J. Comput. Assist. Tomogr. 2003; 27(6):825–846. [PubMed: 14600447]
42. Dixon WT. Simple proton spectroscopic imaging. Radiology. 1984; 153:189–194. [PubMed: 6089263]
43. Seo SW, Kwon JW, Jang SW, Jang SP, Park YS. Feasibility of whole-body MRI for detecting metastatic myxoid liposarcoma: a case series. Orthopedics. 2011; 34(11):e748–54. [PubMed: 22049957]
44. Costelloe CM, Kundra V, Ma J, Chasen BA, Rohren EM, Bassett RL Jr, Madewell JE. Fast dixon whole-body MRI for detecting distant cancer metastasis: a preliminary clinical study. J Magn Reson Imaging. 2012; 35(2):399–408. [PubMed: 21990095]
45. Manenti G, Cicciò C, Squillaci E, Strigari L, Calabria F, Danieli R, Schillaci O, Simonetti G. Role of combined DWIBS/3D-CE-T1w whole-body MRI in tumor staging: Comparison with PET-CT. Eur J Radiol. Sep 9.2011
46. MacDonald LR, Kohlmyer S, Liu C, Lewellen TK, Kinahan PE. Effects of MR surface coils on PET quantification. Med Phys. 2011; 38(6):2948–56. [PubMed: 21815368]
47. Delso G, Martinez-Möller A, Bundschuh RA, Ladebeck R, Candidus Y, Faul D, Ziegler SI. Evaluation of the attenuation properties of MR equipment for its use in a whole-body PET/MR scanner. Phys Med Biol. 2010; 55(15):4361–74. [PubMed: 20647598]
48. Tellmann L, Quick HH, Bockisch A, Herzog H, Beyer T. The effect of MR surface coils on PET quantification in whole-body PET/MR: results from a pseudo-PET/MR phantom study. Med Phys. 2011; 38(5):2795–805. [PubMed: 21776816]
49. Qi J, Leahy RM. Iterative reconstruction techniques in emission computed tomography. Physics in medicine and biology. 2006; 51(15):R541–578. [PubMed: 16861768]
50. Leahy R, Yan X. Incorporation of anatomical MR data for improved functional imaging with PET. Lect. Notes Comput.Sci. 1991; 511:105–120.
51. Bowsher JE, Johnson VE, Turkington TG, et al. Bayesian reconstruction and use of anatomical a priori information for emission tomography. IEEE Trans.Med.Imaging. 1996; 15:673–86. [PubMed: 18215949]
52. Wang CH, Chen JC, Kao CM, Liu RS. Incorporation of correlated MR images in MAP reconstruction of PET images. The Journal of Nuclear Medicine. May.2003 44(5):278.
53. Vriens D, Visser EP, de Geus-Oei LF, Oyen WJ. Methodological considerations in quantification of oncological FDG PET studies. Eur J Nucl Med Mol Imaging. 2010; 37(7):1408–25. [PubMed: 19936745]
54. Tsoumpas C, Mackewn JE, Halsted P, King AP, Buerger C, Totman JJ, Schaeffter T, Marsden PK. Simultaneous PET-MR acquisition and MR-derived motion fields for correction of non-rigid motion in PET. Ann Nucl Med. 2010; 24(10):745–50. [PubMed: 20842466]
55. Picard Y, Thompson CJ. Motion correction of PET images using multiple acquisition frames. IEEE Trans Med Imaging. 1997; 16(2):137–144. [PubMed: 9101323]

56. Haacke, EM.; Brown, RW.; Thompson, MR.; Venkatesan, R. Magnetic Resonance Imaging: Physical Principles and Sequence Design. Wiley-Liss; New York: 1999.
57. King AP, Buerger C, Tsoumpas C, Marsden PK, Schaeffter T. Thoracic respiratory motion estimation from MRI using a statistical model and a 2-D image navigator. Med Image Anal. 2012; 16(1):252–64. [PubMed: 21959365]
58. Guérin B, Cho S, Chun SY, Zhu X, Alpert NM, El Fakhri G, Reese T, Catana C. Nonrigid PET motion compensation in the lower abdomen using simultaneous tagged-MRI and PET imaging. Med Phys. 2011; 38(6):3025–38. [PubMed: 21815376]
59. Gambhir, SS. Quantitative assay development for PET. In: Phelps, ME., editor. PET Molecular Imaging and its Biological Applications. Springer; New York: 2004. p. 125-217.
60. Adam LE, Karp JS, Daube-Witherspoon ME, Smith RJ. Performance of a whole-body PET scanner using curve-plate NaI(Tl) detectors. J Nucl Med. 2001; 42:1821–1830. [PubMed: 11752080]
61. Zaidi H, Ojha N, Morich M, et al. Design and performance evaluation of a whole-body Ingenuity TF PET-MRI system. Phys Med Biol. 2011; 56:3091–3106. [PubMed: 21508443]
62. Hoffman EJ, Huang SC, Phelps ME. Quantitation in positron emission computed tomography: 1. Effect of object size. J Comput Assist Tomogr. 1979; 3:299–308. [PubMed: 438372]
63. Mazziotta JC, Phelps ME, Plummer D, Kuhl DE. Quantitation in positron emission computed tomography: 5. Physical-anatomical effects. J Comput Assist Tomogr. 1981; 5:734–743. [PubMed: 6975289]
64. Greuter HN, Boellaard R, van Lingen A, Franssen EJ, Lammertsma AA. Measurement of18 F-FDG concentrations in blood samples: comparison of direct calibration and standard solution methods. J Nucl Med Technol. 2003; 31:206–209. [PubMed: 14657286]
65. de Geus-Oei LF, Visser EP, Krabbe PF, et al. Comparison of image-derived and arterial input functions for estimating the rate of glucose metabolism in therapy-monitoring 18F-FDG PET studies. J Nucl Med. 2006; 47:945–949. [PubMed: 16741303]
66. Muller-Gartner HW, Links JM, Prince JL, et al. Measurement of radiotracer concentration in brain gray matter using positron emission tomography: MRI-based correction for partial volume effects. J Cereb Blood Flow Metab. 1992; 12:571–583. [PubMed: 1618936]
67. Rousset OG, Ma Y, Evans AC. Correction for partial volume effects in PET: Principle and validation. J Nucl Med. 1998; 39:904–911. [PubMed: 9591599]
68. Boussion N, Hatt M, Lamare F, Bizais Y, Turzo A, Cheze-LeRest C, Visvikis D. A multiresolution image based approach for correction of partial volume effects in emission tomography. Phys Med Biol. 2006; 51(7):1857–76. [PubMed: 16552110]
69. Meltzer CC, Kinahan PE, Greer PJ, et al. Comparative evaluation of MR-based partial volume correction schemes for PET. J Nucl Med. 1999; 40:2053–2065. [PubMed: 10616886]
70. Shidahara M, Tsoumpas C, Hammers A, Boussion N, Visvikis D, Suhara T, Kanno I, Turkheimer FE. Functional and structural synergy for resolution recovery and partial volume correction in brain PET. Neuroimage. 2009; 44(2):340–8. [PubMed: 18852055]
71. Torres Martin de Rosales R, Tavaré R, Paul RL, Jauregui-Osoro M, Protti A, Glaria A, Varma G, Szanda I, Blower PJ. Synthesis of 64Cu(II)-bis(dithiocarbamatebisphosphonate) and its conjugation with superparamagnetic iron oxide nanoparticles: in vivo evaluation as dual-modality PET-MRI agent. Angew Chem Int Ed Engl. 2011; 50(24):5509–13. [PubMed: 21544908]
72. Glaus C, Rossin R, Welch MJ, Bao G. In vivo evaluation of (64)Cu-labeled magnetic nanoparticles as a dual-modality PET/MR imaging agent. Bioconjug Chem. 2010; 21(4):715–22. [PubMed: 20353170]
73. Choi, J.-s; Park, J.; Nah, H.; Woo, S.; Oh, J.; Kim, K.; Cheon, G.; Chang, Y.; Yoo, J.; Cheon, JA. Hybrid Nanoparticle Probe for Dual-Modality Positron Emission Tomography and Magnetic Resonance Imaging. Angewandte Chemie International Edition. 2008; 47:6259–6262.
74. Lee HY, Li Z, Chen K, Hsu AR, Xu C, Xie J, Sun S, Chen XJ. PET/MRI dual-modality tumor imaging using arginine-glycine-aspartic (RGD)-conjugated radiolabeled iron oxide nanoparticles. Nucl Med. 2008; 49(8):1371–9.
75. Gaertner FC, Schwaiger M, Beer AJ. Molecular imaging of αvß3 expression in cancer patients. Q J Nucl Med Mol Imaging. 2010; 54(3):309–26. [PubMed: 20639816]

76. Frullano L, Catana C, Benner T, Sherry A, Caravan P. Bimodal MR-PET Agent for Quantitative pH Imaging. Angewandte Chemie. 2010; 122:2432–4.
77. Vees H, Senthamizhchelvan S, Miralbell R, Weber D, Ratib O, Zaidi H. Assessment of various strategies for 18F-FET PET-guided delineation of target volumes in high-grade glioma. Eur. J. Nucl. Med. Mol. Imaging. 2009; 36(2):182–193. [PubMed: 18818918]
78. Thorwarth D, Henke G, Müller AC, Reimold M, Beyer T, Boss A, Kolb A, Pichler B, Pfannenberg C. Simultaneous 68Ga-DOTATOC-PET/MRI for IMRT treatment planning for meningioma: first experience. Int J Radiat Oncol Biol Phys. 2011; 81:277–83. [PubMed: 21300465]
79. Huang SH, Chien CY, Lin WC, Fang FM, Wang PW, Lui CC, Huang YC, Hung BT, Tu MC, Chang CC. A comparative study of fused FDG PET/MRI, PET/CT, MRI, and CT imaging for assessing surrounding tissue invasion of advanced buccal squamous cell carcinoma. Clin Nucl Med. 2011; 36:518–25. [PubMed: 21637051]
80. Tatsumi M, Isohashi K, Onishi H, Hori M, Kim T, Higuchi I, Inoue A, Shimosegawa E, Takeda Y, Hatazawa J. 18 F-FDG PET/MRI fusion in characterizing pancreatic tumors: comparison to PET/CT. Int J Clin Oncol. 2011; 16:408–15. [PubMed: 21347626]
81. Moy L, Noz ME, Maguire GQ Jr, Melsaether A, Deans AE, Murphy-Walcott AD, Ponzo F. Role of fusion of prone FDG-PET and magnetic resonance imaging of the breasts in the evaluation of breast cancer. Breast J. 2010; 16:369–76. [PubMed: 20443788]
82. Jansen JF, Schöder H, Lee NY, Wang Y, Pfister DG, Fury MG, Stambuk HE, Humm JL, Koutcher JA, Shukla-Dave A. Noninvasive assessment of tumor microenvironment using dynamic contrast-enhanced magnetic resonance imaging and 18F-fluoromisonidazole positron emission tomography imaging in neck nodal metastases. Int J Radiat Oncol Biol Phys. 2010; 77(5):1403–10. [PubMed: 19906496]
83. Cho H, Ackerstaff E, Carlin S, Lupu ME, Wang Y, Rizwan A, O'Donoghue J, Ling CC, Humm JL, Zanzonico PB, Koutcher JA. Noninvasive multimodality imaging of the tumor microenvironment: registered dynamic magnetic resonance imaging and positron emission tomography studies of a preclinical tumor model of tumor hypoxia. Neoplasia. 2009; 11(3):247–59. [PubMed: 19242606]
84. Zhang F, Zhu L, Liu G, Hida N, Lu G, Eden HS, Niu G, Chen X. Multimodality imaging of tumor response to doxil. Theranostics. 2011; 1:302–9. [PubMed: 21772927]
85. Atuegwu NC, Gore JC, Yankeelov TE. The integration of quantitative multi-modality imaging data into mathematical models of tumors. Phys Med Biol. May 7; 2010 55(9):2429–49. [PubMed: 20371913]
86. Hricak H, Amparo EG. Body MRI: Alleviation of claustrophobia by prone positioning. Radiology. 1984; 152:819. [PubMed: 6463267]
87. Quirk ME, Letendre AJ, Ciottone RA, Lingley JF. Evaluation of three psychologic interventions to reduce anxiety during MR imaging. Radiology. 1989; 173:759–762. [PubMed: 2682775]
88. Quirk ME, Letendre AJ, Ciottone RA, Lingley JF. Anxiety in patients undergoing MR imaging. Radiology. 1989; 170:463–466. [PubMed: 2911670]
89. Flaherty JA, Hoskinson K. Emotional Distress during Magnetic Resonance Imaging. N Engl J Med. 1989; 320:467–468. [PubMed: 2913515]
90. Meléndez JC, McCrank E. Anxiety-related reactions associated with magnetic resonance imaging examinations. JAMA. 1993; 270(6):745–7. [PubMed: 8336378]
91. Katz RC, Wilson L, Frazer N. Anxiety and its determinants in patients undergoing magnetic resonance imaging. J Behav Ther Exp Psychiatry. 1994; 25(2):131–4. [PubMed: 7983222]
92. Kieran J, Murphy, James A. Brunberg. Adult claustrophobia, anxiety and sedation in MRI. Magnetic Resonance Imaging. 1997; 15(1):51–54. [PubMed: 9084025]
93. Sharon M, Hamblen CNMT, Val J, Lowe MD. Clinical 18F-FDG Oncology Patient Preparation Techniques. J. Nucl. Med. Technol. 2003; 31(1):3–10. [PubMed: 12624120]
94. Mawlawi, Osama; Kappadath, SC.; Pan, Tinsu; Rohren, Eric; Macapinlac, Homer A. Factors Affecting Quantification in PET/CT Imaging. Current Medical Imaging Reviews. 2008; 4(1):34–45.
95. Cohade C, Osman M, Pannu HK, Wahl RL. Uptake in supraclavicular area fat ("USA-Fat"): description on 18F-FDG PET/CT. J Nucl Med. 2003; 44:170–176. [PubMed: 12571205]

96. Yeung HW, Grewal RK, Gonen M, Schoder H, Larson SM. Patterns of [18]F FDG uptake in adipose tissue and muscle: a potential source of false-positives for PET. J Nucl Med. 2003; 44:1789–1796. [PubMed: 14602861]

97. McQuattie S. Pediatric PET/CT Imaging: Tips and Techniques. J. Nucl. Med. Technol. 2008; 36:171–178. [PubMed: 19008284]

98. Veitch TA. Pediatric nuclear medicine, part I: developmental cues. J Nucl Med Technol. 2000; 28:3–7. [PubMed: 10763774]

99. Eisenhauer EA, Therasse P, Bogaerts J, Schwartz LH, Sargent D, Ford R, Dancey J, Arbuck S, Gwyther S, Mooney M, Rubinstein L, Shankar L, Dodd L, Kaplan R, Lacombe D, Verweij J. New response evaluation criteria in solid tumours: revised RECIST guideline (version 1.1). Eur J Cancer. 2009; 45(2):228–47. [PubMed: 19097774]

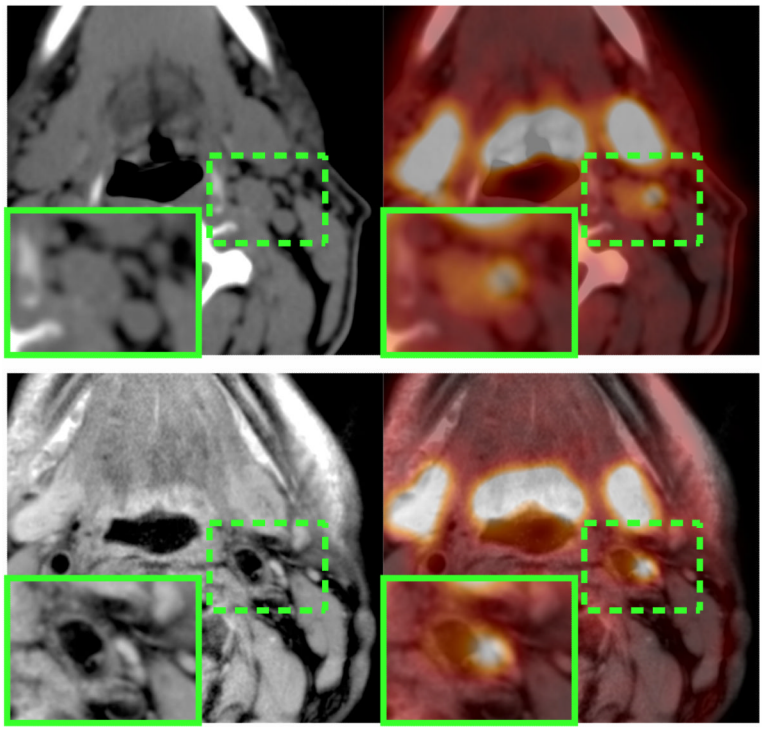

Fig. 1.

PET/CT (top row) vs. PET/MR (bottom row) of a patient with an inflamed plaque. Higher soft-tissue contrast of the MR image (bottom left) compared to the CT image (top left) allows better delineation of the luminal area and therefore improves quantification of the PET uptake signal.

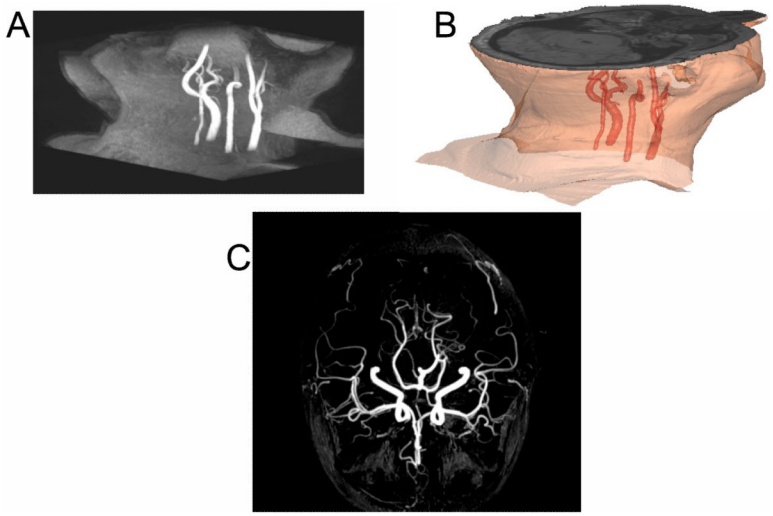

Fig. 2.

Use of MR time-of-flight (ToF) sequence to highlight the arterial blood pool. (A) 3D-ToF on neck region and 3D image reconstruction after arterial segmentation (B). (C) MR-angiography of the brain using time-of-flight (ToF) MR sequence.

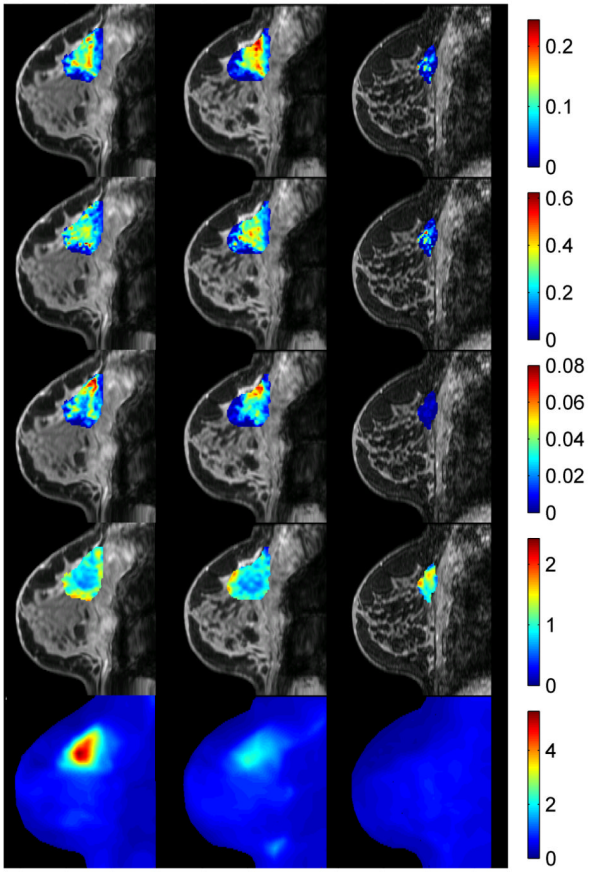

Fig. 3.

A retrospectively registered PET-MRI approach to monitoring neoadjuvant chemotherapy (NAC) in an invasive ductal carcinoma. Specifically, quantitative DCE- and DW-MRI parameters have been registered to an FDG-PET scan at three time points during NAC: 1) pre-therapy (column 1), 2) after one cycle of therapy (column 2), and 3) at the conclusion of NAC but prior to surgery (column 3). The first three rows present data available from the MRI study: K^{trans}, v_e, v_p, and ADC, respectively. The final row presents the FDG-PET map at each time point. The ability to simultaneously acquire such rich data provides the opportunity for many studies described in the text.